OUTLINE OF E-DEFENSE SHAKING TABLE TESTS FOR SEMI-ACTIVE CONTROL OF BASE-ISOLATION SYSTEM

E. Sato[(1)], A. Kishida[(2)], K. Kajiwara[(3)], H.Fujitani[(4)], Y.Mukai[(5)],
M. Ito[(6)], K. Itahara[(7)], S. Iba[(8)], E. A. Johnson[(9)], R. Christenson[(10)]

[(1)] *Researcher, National Research Institute for Earth Science and Disaster Resilience, eiji@bosai.go.jp*
[(2)] *Researcher, National Research Institute for Earth Science and Disaster Resilience, akiko_kishida@bosai.go.jp*
[(3)] *Researcher, National Research Institute for Earth Science and Disaster Resilience, kaji@bosai.go.jp*
[(4)] *Professor, Kobe University, fujitani@kobe-u.ac.jp*
[(5)] *Professor, Kobe University, ymukai@port.kobe-u.ac.jp*
[(6)] *Researcher, Building Research Institute, mai_ito@kenken.go.jp*
[(7)] *Student, Kobe University, 185t005t@stu.kobe-u.ac.jp*
[(8)] *Student, Kobe University, 180t008t@stu.kobe-u.ac.jp*
[(9)] *Professor, University of Southern California, JohnsonE@usc.edu*
[(10)] *Professor, University of Connecticut, richard.christenson@uconn.edu*

Abstract

When an earthquake occurs, semi-active seismic isolation structures with designed controllers have the potential to reduce deformations significantly more than passive seismic isolation structures. In this study, shaking table tests for a semi-active isolation structure using a variable damper were conducted in an effort determine if excessive deformation of base-isolation systems could be prevented under near-fault pulse ground motions such as those occurring at JR Takatori Station during the 1995 Southern Hyogo Prefecture Earthquake and in Sylmar during the 1994 Northridge, California Earthquake. The steel frame semi-active isolation structure used in this study was 7 m long, 5.5 m wide, 2.3 m high, and weighed about 14.9 t. The superstructure was supported by linear guides, and a natural rubber bearing was set between the superstructure and the shaking table. A magnetorheological (MR) fluid damper was used to apply variable dampening. The target responses of the superstructure were realized by controlling the damping force of the MR damper. During the first part of the study, characteristic tests of the MR damper were conducted, and its responses were modeled from those results. Next, the shaking table tests were conducted to create a system identification of the isolation structure. From these results, various semi-active controllers were designed for the isolation system, and the isolation performance of the targeted semi-active isolation system was then evaluated using shaking tests for various earthquake ground motions. All the tests in this study were performed at "E-Defense" 3-D Full-Scale Earthquake Testing Facility located in Miki City, Hyogo Prefecture, which is operated by the National Research Institute for Earth Science and Disaster Resilience (NIED). This paper describes the MR damper, the semi-active isolation system, and the experimental methods used for those shaking tests.

Keywords: semi-active seismic isolation; shaking table test; MR damper; E-Defense

1. Introduction

It is possible that even advanced seismic isolation structures could experience large deformations in their isolation layers during certain earthquake ground motions. In such cases, structures equipped with semi-active controls are thought to be capable of not only reducing the effects of such deformations but also reducing response acceleration needed to maintain the functions of the structures [1]. Therefore, in order to evaluate the performance of a seismic isolation structure using a magnetorheological (MR) fluid damper [2] equipped with semi-active controls, various large-scale shaking table tests were conducted at E-Defense [3]. In this paper, the MR damper, the semi-active isolation system, the experimental methods used for the shaking tests, and other related factors are reported [4,5,6,7,8,9].

2. Semi-active Seismic Isolation Test Specimen

Fig. 1 shows a photograph of the test specimen used for semi-active seismic isolation shaking tests installed on E-Defense, whereas Fig. 2 shows a schematic drawing of the test specimen.

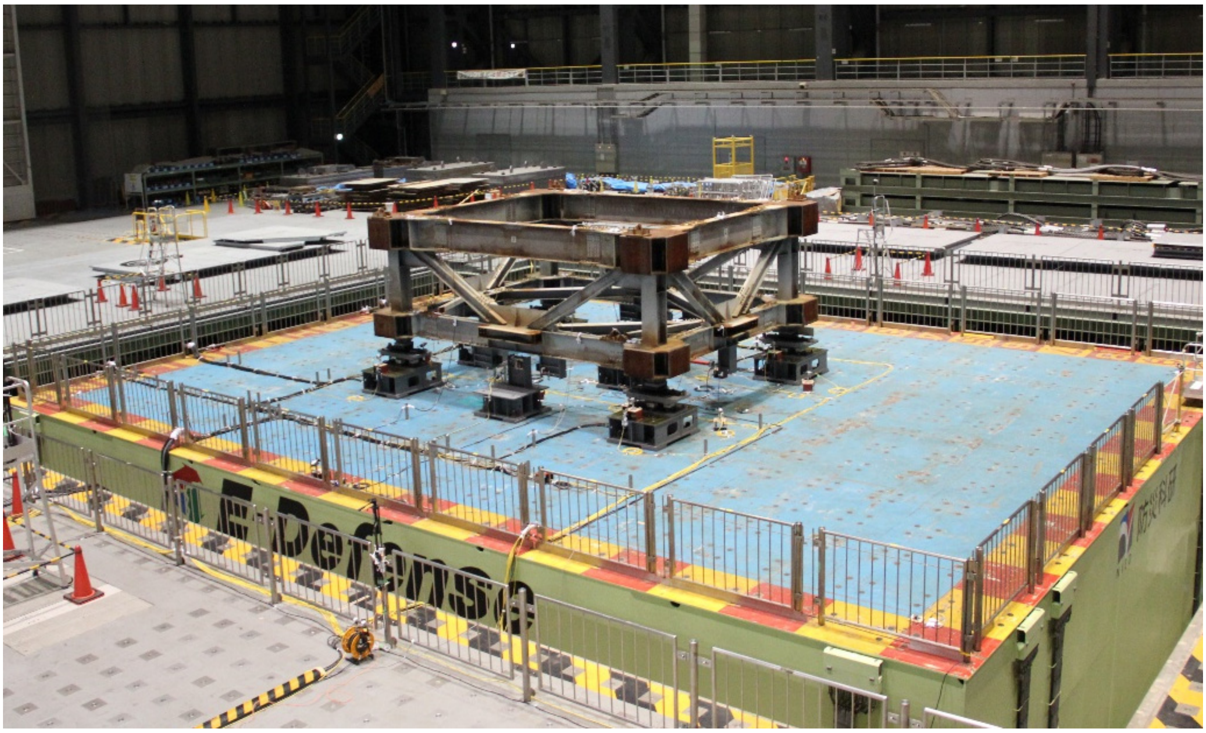

Fig. 1 – Semi-active seismic isolation test specimen

The test specimen used in this study was 7 m long, 5.5 m wide, 2.3 m high, and weighed about 14.9 t. The actual superstructure [10] was a 1 × 1 span steel frame structure supported by H300 steel beam columns at the four corners and V-shaped braces installed at each of the four sides. Therefore, the superstructure can be treated as a configuration with sufficient rigidity for testing in a seismic isolation system.

The seismic isolation system provides horizontal one-way seismic isolation. The superstructure was supported by four linear guides. A natural rubber bearing was installed at the beam center in the width direction, and an MR damper was installed on the opposite side of the beam. Semi-active seismic isolation was achieved by controlling the dampening force of the MR damper. The allowable displacement of the seismic isolation system was ± 250 mm.

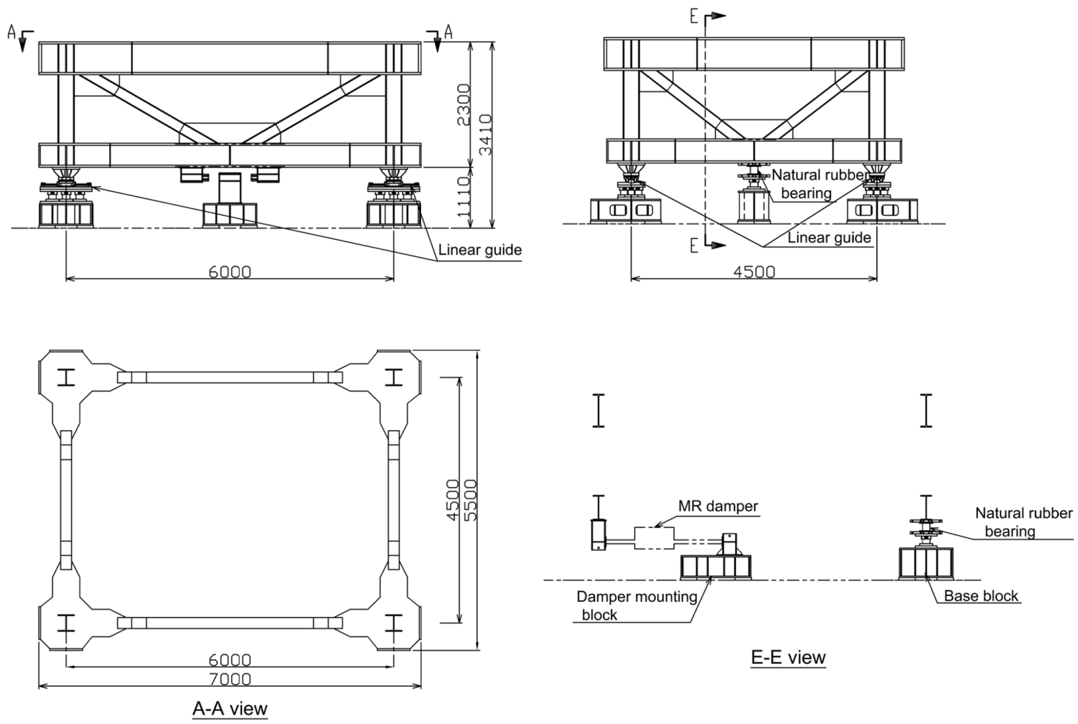

Fig. 2 – Schematic drawing of semi-active seismic isolation test specimen

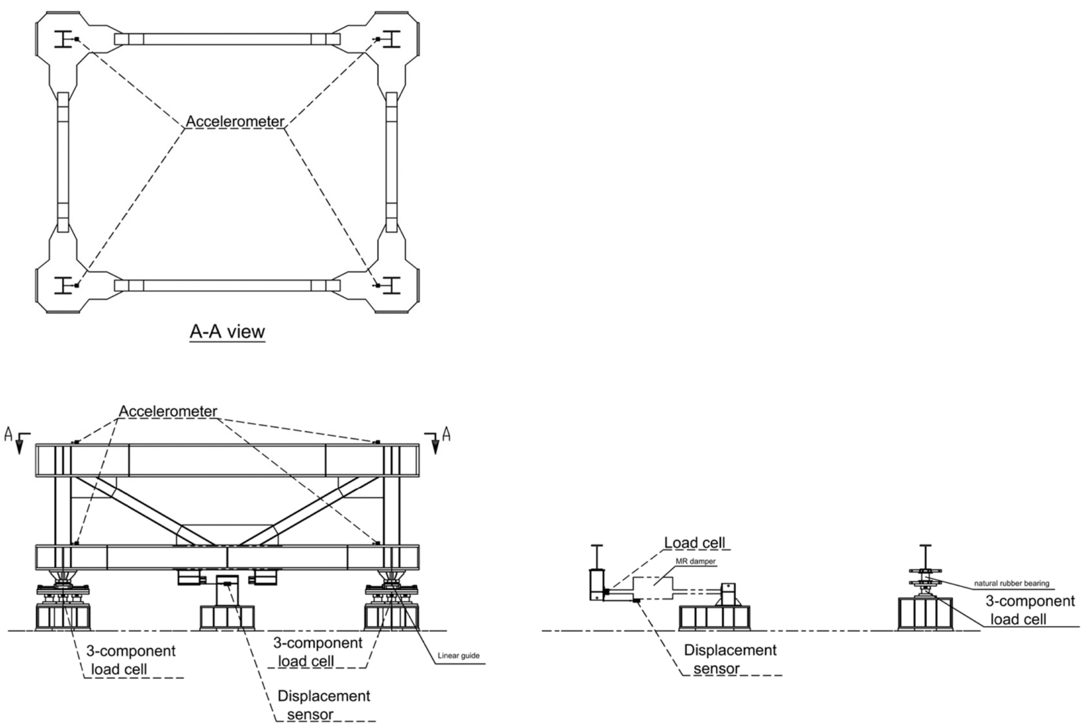

Fig. 3 – Sensor arrangement

3. Measurements

Various measurement values including input acceleration, superstructure response acceleration, isolation layer displacement, natural rubber bearing load, MR damper load, and linear guide load were collected during the semi-active seismic isolation system shaking table tests. Fig. 3 shows the arrangement of the main measurement sensors. The natural rubber bearing load was measured by installing a three-component load cell below the natural rubber bearing, whereas the linear guide load was measured by installing four three-component load cells below the linear guides, as shown in Fig. 4.

The MR damper load was measured by installing a load cell at the tip of the MR damper rod, while a magnetostrictive displacement meter was used to measure both the displacement and velocity of the MR damper rod during testing.

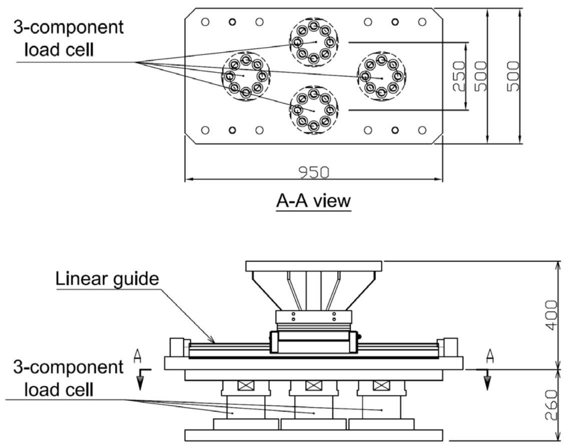

Fig. 4 – Arrangement of four three-component load cells for linear guide load

4. Test specimen characteristics

4.1 Natural rubber bearing

Table 1 shows the production specifications of the natural rubber bearing, and Fig. 5 shows the displacement-load hysteresis of the bearing when it was excited by sine waves with a period of 2, 3, and 4 s. From these results, the natural rubber bearing stiffness was estimated to be 42.3 kN/m, which is harder than the production specification, and the seismic isolation period of the test specimen was calculated to be about 3.7 s.

Table 1 – Natural rubber bearing production specifications

Item	Standard value
Rubber outer diameter (mm)	128
Rubber thickness (mm)	12.5
Number of rubber layers	8
Rubber total thickness (mm)	100
Internal steel plate thickness (mm)	2.0
Rubber material	G 0.28
Shear modulus (N/mm^2)	0.28
Primary stiffness (kN/m)	-
Secondary stiffness (kN/m)	38.5
Critical strain (%), critical deformation (mm)	400, 400 or more

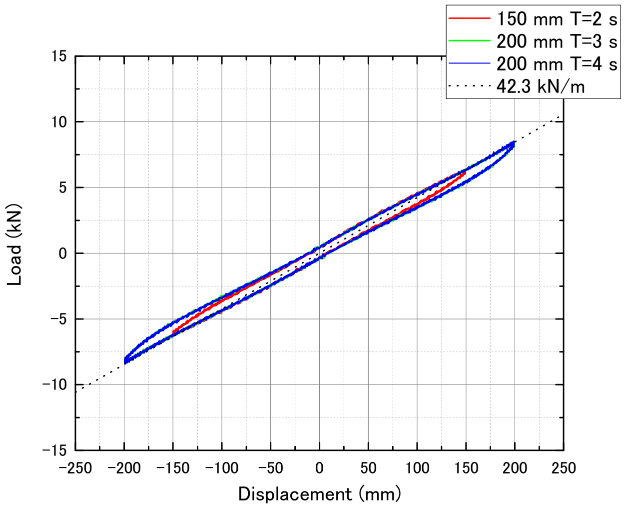

Fig. 5 – Displacement-load hysteresis of natural rubber bearing during sine wave excitation

Fig. 6 shows the displacement-load hysteresis for the natural rubber bearing during the shaking table tests. Here, it can be seen that the bearing stiffness is almost the same as during the sine wave excitation tests.

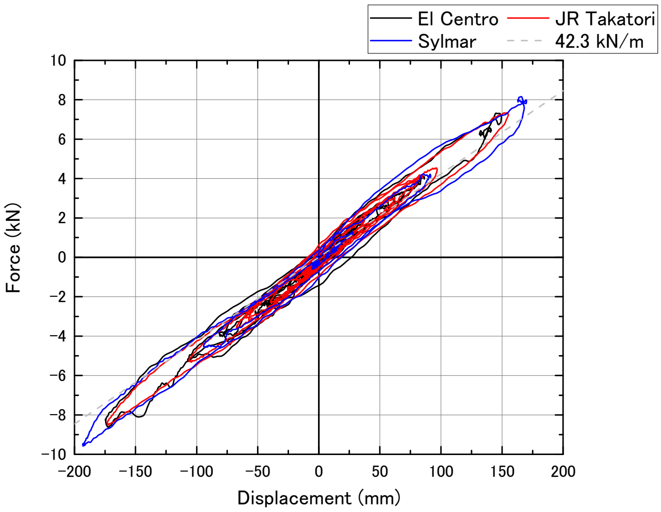

Fig. 6 – Displacement-load hysteresis of natural rubber bearing during shaking table tests

4.2 Linear guides

Fig. 7 and Fig. 8 show the hysteresis for the linear guides during the shaking table tests. More specifically, Fig. 7 shows the results when the input is a small level random waveform, and the relative displacement is small, while Fig. 8 shows the results using the artificial BCJ-L2 seismic waveform. When the displacement is small, the load characteristics of the linear guides correspond to stable friction. However, they are slightly unstable during the large seismic wave shaking table tests. Using these results, the total friction force for the linear guides could be estimated at approximately 3 to 4 kN.

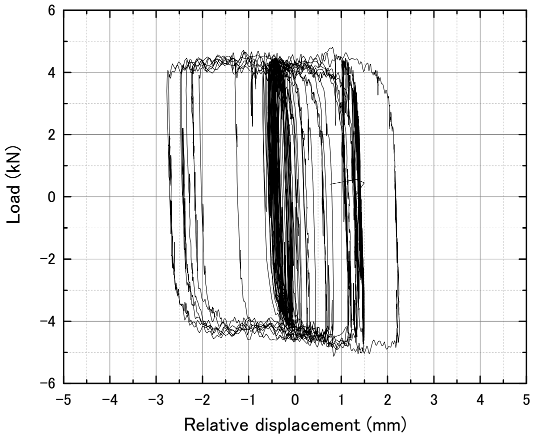

Fig. 7 – Displacement-load hysteresis for linear guides during small random wave

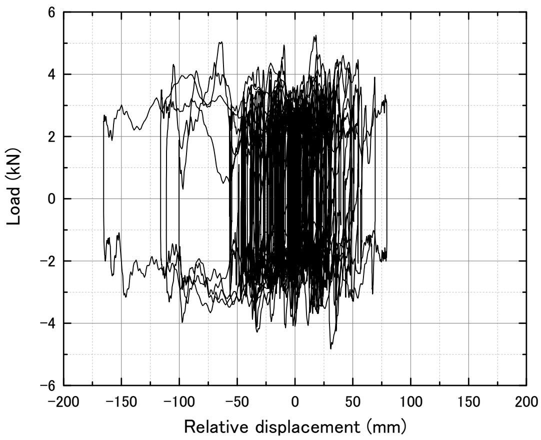

Fig. 8 – Displacement-load hysteresis for linear guides during BCJ-L2 seismic wave

4.3 MR damper

The MR damper uses a magnetorheological fluid and controls the damping force by changing the current applied to the coil, which then changes the coil's magnetic field. In order to confirm the performance of the MR damper, unit excitation tests of the device were conducted. In these tests, the MR damper was loaded with sine waves input by an actuator, and various data were recorded. Fig. 9 shows the load displacement and load velocity relationships for the MR damper. From those results, it was confirmed that the MR damper could be modeled using a Bingham plastic model that includes a dashpot and a friction element in parallel. Hence, the controllable force of the MR damper was obtained by the Bingham plastic model expressed by Eq. (1).

$$F_{MR} = (-0.171I^2 + 2.522I - 0.247)sgn(\dot{x}_t) + (0.501I + 0.859)\dot{x}_t \quad (1)$$

Here, F_{MR} is the MR damper generation force, I is the applied current, and x_t and $\dot{x}_t$ are the displacement and velocity of the rod, respectively. Fig. 9 also shows the result calculated from Eq. (1). The obtained results show that the experimental and modeling results are in good agreement, which confirms the validity of the model.

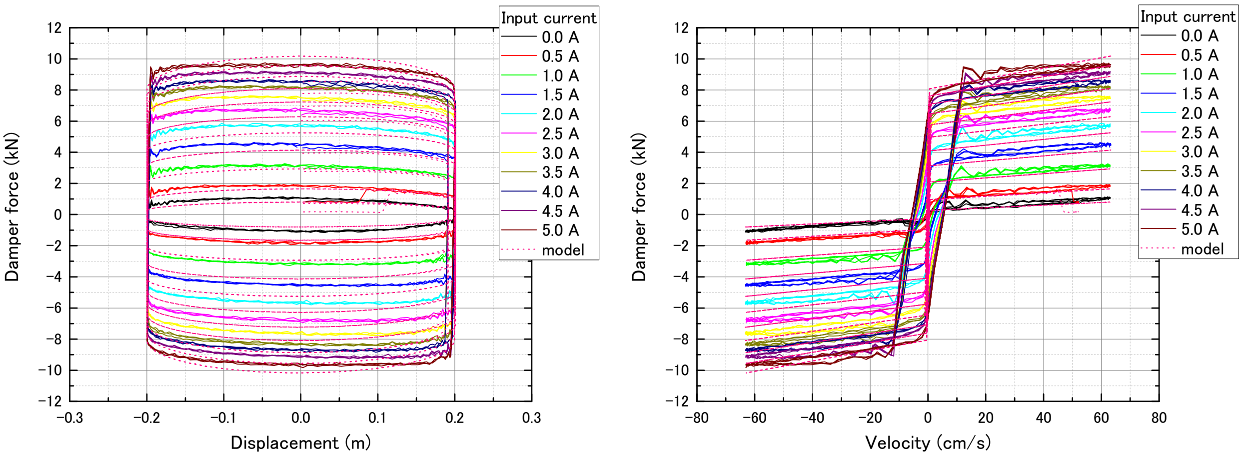

(a) Load displacement relationship (b) Load velocity relationship

Fig. 9 – MR damper characteristics (including the Bingham plastic model)

5. Input ground motion

Shaking table tests were conducted with one horizontal direction excitation. The input ground motions were the El Centro NS waveform (El Centro) recorded during the 1940 Imperial Valley earthquake, the JR Takatori Station NS waveform [11] (JR Takatori) recorded during the 1995 Southern Hyogo Prefecture earthquake, and the Sylmar NS waveform (Sylmar) recorded during the 1994 Northridge earthquake. The input level was set at 150% for El Centro, 40% for JR Takatori, and 50% for Sylmar in consideration of the allowable displacement of the seismic isolation system. The seismic intensity of all input ground motions was set at 6-Lower based on the Japan Meteorological Agency measurement scale. Fig. 10 shows the time histories of the input ground motions, and Fig. 11 shows the acceleration response spectra.

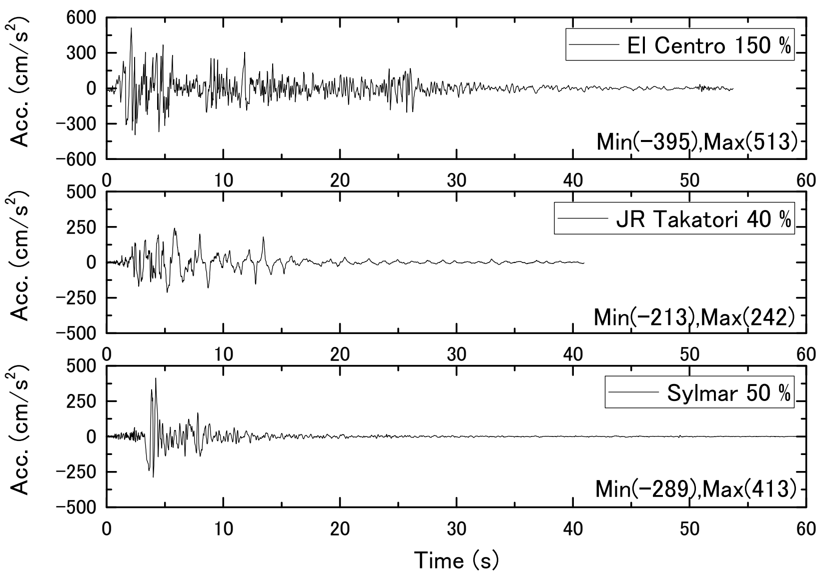

Fig. 10 – Time histories of input ground motions

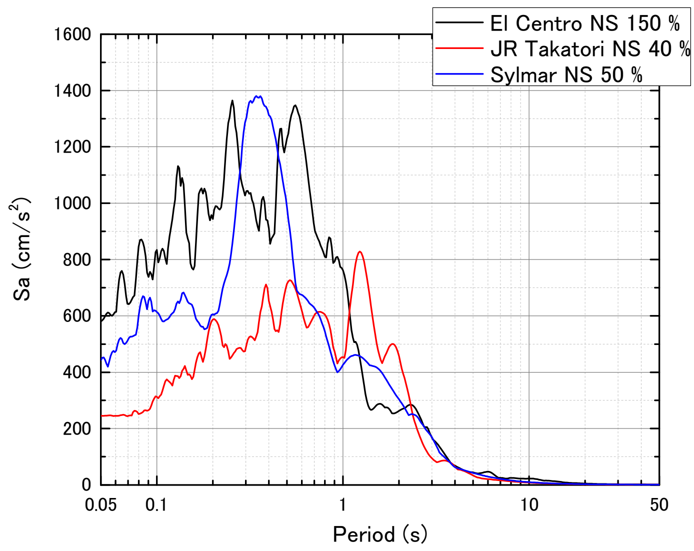

Fig. 11 – Acceleration response spectra for input ground motions

6. Shaking table tests

E-Defense shaking table tests were conducted using the semi-active seismic isolation test specimen described above. In these tests, various semi-active controls were used for the MR damper, and the results obtained were compared to the input current when the MR damper was fixed. In order to confirm the dynamic characteristics of the seismic isolation test specimen, a Bode diagram of the test specimen response acceleration occurring when the MR damper input current was constant is shown in Fig. 12. From these amplitude characteristics, it can be seen that the seismic isolation period was around 3 s. It should be noted that this period is shorter than the result calculated from the characteristics of each member, probably because the seismic isolation period could not be accurately identified in these tests due to the unstable friction characteristics of the linear guides.

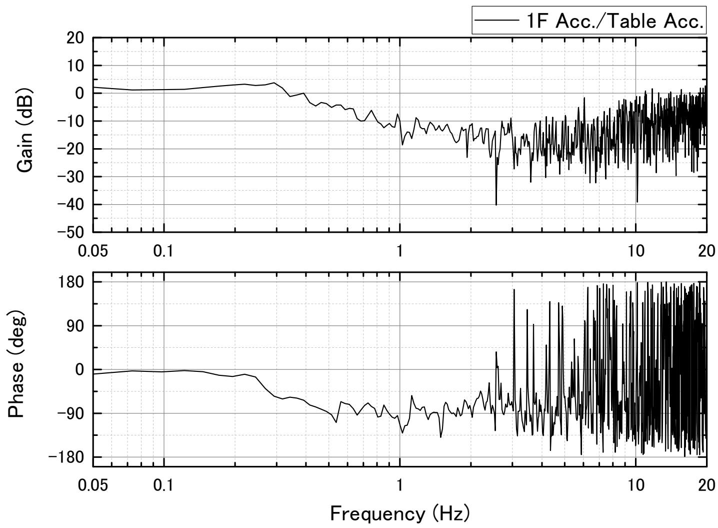

Fig. 12 – Dynamic characteristics of seismic isolation test specimen (Bode diagram)

Fig. 13 shows the acceleration response spectra for the input waveform during the shaking table in the first and last tests. This figure also shows the response spectra for the target input waveform. The results indicate that the input waveform of the shaking table accurately matches the target input waveform In the shaking table tests using other semi-active controls, the input waveform also coincides with the target waveform. Therefore, the input conditions to the semi-active seismic isolation test specimen in each shaking table test can be considered nearly the same.

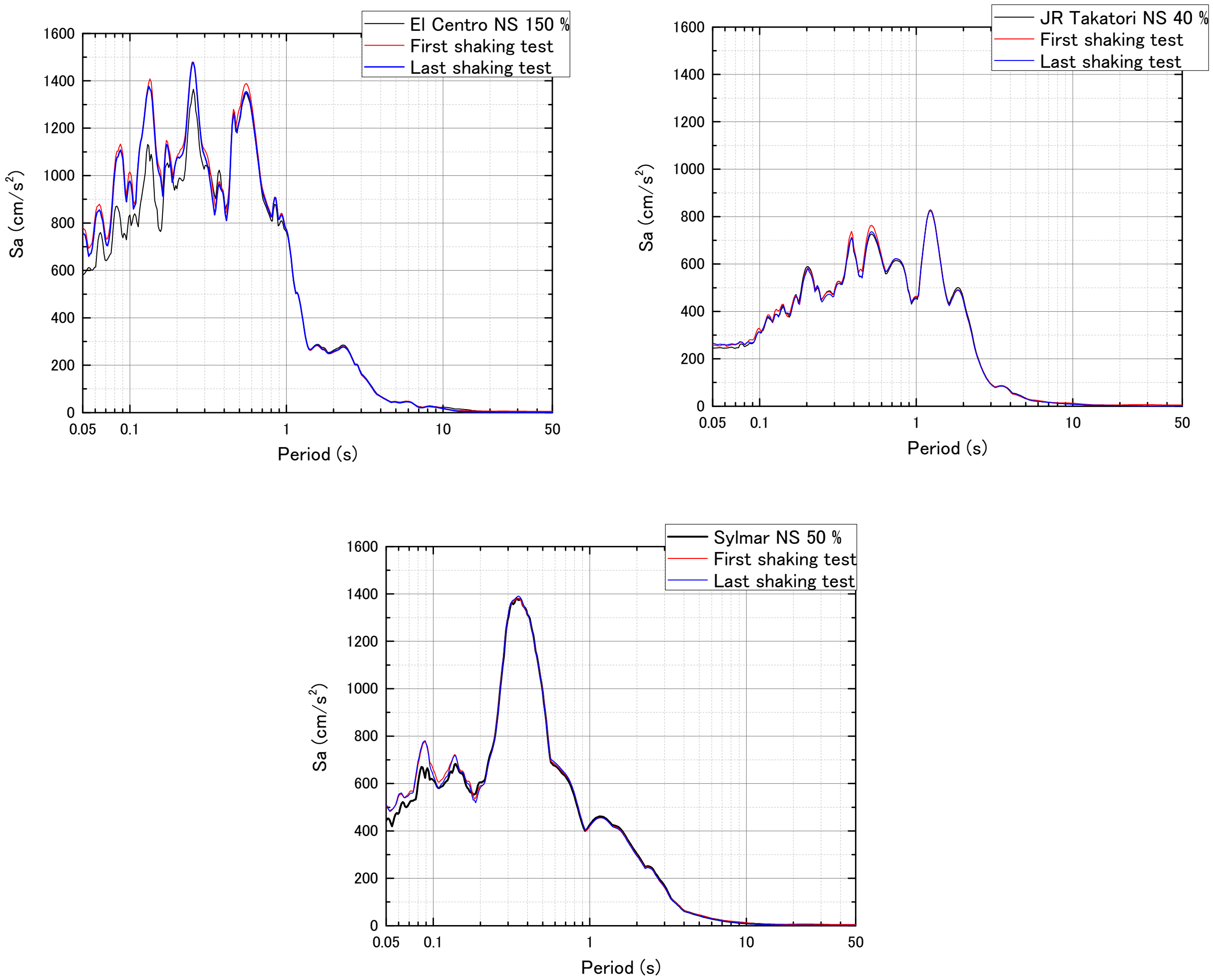

Fig. 13 – Acceleration response spectra for input waves on shaking table and target wave

7. Conclusion

In this paper, we reported on the test specimen, measurement methods, and table test conditions used during shaking table tests for semi-active seismic isolation structures at NIED "E-Defense" 3-D Full-Scale Earthquake Testing Facility. We also confirmed that the input conditions were the same in each semi-active seismic isolation test. The in-depth details of each semi-active seismic isolation test will be reported in other papers.

8. Acknowledgements

This work was supported by JSPS Grant No. R2904 in the Program for Fostering Globally Talented Researchers and the research unit of Multidisciplinary Integration for Resilience and Innovation (MIRAI) in Kobe University.

9. References

[1] Eiji SATO, Takafumi FUJITA, (2007): Semi-active Seismic Isolation System with Controllable Friction Dampers Using Piezoelectric Actuators, *Journal of Environment and Engineering*, Volume 2 Issue 2 Pages 215-226.

[2] Katsuaki Sunakoda, Hiroshi Sodeyama, Norio Iwata, Hideo Fujitani, Satsuya Soda, (2000): Dynamic characteristics of magneto-rheological fluid damper, *Proc. SPIE 3989, Smart Structures and Materials 2000: Damping and Isolation.*

[3] Keiichi Ohtani, Nobuyuki Ogawa, Tsuneo Katayama, Heki Shibata, (2004): CONSTRUCTION OF E-DEFENSE (3-D FULL-SCALE EARTHQUAKE TESTING FACILITY), *Proceedings of 13th World Conference on Earthquake Engineering*, Paper N° 189.

[4] K. Itahara, H. Fujitani, Y. Mukai, M. Ito, E. Sato, S. Iba, (2020): SHAKING TABLE TEST AND REAL-TIME HYBRID SIMULATION IN SEMI-ACTIVE CONTROLLED BASE-ISOLATION SYSTEM. *Proceedings of 17th World Conference on Earthquake Engineering*, Paper N° C001668.

[5] A. Kishida, E. Sato, S. Iba, H. Fujitani, Y. Mukai, K. Itahara, E. A. Johnson, K. Kajiwara, (2020): SEMI-ACTIVE CONTROL OF BASE-ISOLATED STRUCTURE USING MR DAMPER THAT SIMULATES VARIABLE HYDRAULIC DAMPER AND COMPLEX STIFFNESS DAMPER. *Proceedings of 17th World Conference on Earthquake Engineering*, Paper N° C001644.

[6] M. Ito, H. Fujitani, Y. Mukai, E. Sato, E. A. Johnson, R. Christenson, A. Kishida, (2020): EVENTUAL SLIDING MODE CONTROL FOR AN ISOLATED STRUCTURE USING MR DAMPER. *Proceedings of 17th World Conference on Earthquake Engineering*, Paper N° C001351.

[7] Q. Fang, E. A. Johnson, E. Sato, H. Fujitani, Y. Mukai, (2020): E-DEFENSE SHAKING TABLE EXPERIMENTS OF CONTROLLABLE DAMPING STRATEGIES FOR A BASE-ISOLATED STRUCTURE. *Proceedings of 17th World Conference on Earthquake Engineering*, Paper N° C003418.

[8] R. Christenson, M. Stevens, E. Sato, H. Fujitani, Y. Mukai, (2020): PERFORMANCE OF SEMI-ACTIVE CONTROLLERS FOR A LARGESCALE BASE-ISOLATION STRUCTURE WITH MR DAMPER. *Proceedings of 17th World Conference on Earthquake Engineering*, Paper N° C003370.

[9] H. Fujitani, Y. Mukai, E. Sato, E. A. Johnson, R. Christenson, A. Kishida, M. Ito, T. Shima, K. Itahara, S. Iba, A. Honma, H. Fukui, (2020): COMPARISON OF E-DEFENSE TEST RESULTS BY FIVE INSTITUTES OF SEMI-ACTIVE CONTROL OF BASE-ISOLATION SYSTEM, *Proceedings of 17th World Conference on Earthquake Engineering*, Paper N° C001612.

[10] Toru Takeuchi, Kazuhiko Kasai, Mitsumasa Midorikawa, Yuichi Matsuoka, Takeshi Asakawa, Isao Kubodera, Yuji Kurokawa, Shoichi Kishiki and Hirotaka Ando, (2008): Shaking table test using E-Defense multipurpose test bed, *Proc., 14th World Conf. on Earthquake Engineering.*

[11] Y. Nakamura, F. Uehan, H. Inoue, (1996): Waveform and its Analysis of the 1995 Hyogo-Ken-Nanbu Earthquake (II), JR Earthquake Information No. 23d, Railway Technical Research Institute, March 1996 (in Japanese)

